MOLECULAR AND CELLULAR BIOLOGY, Oct. 2009, p. 5251–5263 Vol. 29, No. 19
0270-7306/09/$08.00+0 doi:10.1128/MCB.00495-09

# Dual Roles of the Mammalian GARP Complex in Tethering and SNARE Complex Assembly at the *trans*-Golgi Network[▽]

F. Javier Pérez-Victoria and Juan S. Bonifacino*

*Cell Biology and Metabolism Program, Eunice Kennedy Shriver National Institute of Child Health and Human Development, National Institutes of Health, Bethesda, Maryland 20892*

Received 15 April 2009/Returned for modification 8 May 2009/Accepted 8 July 2009

**Tethering factors and SNAREs control the last two steps of vesicular trafficking: the initial interaction and the fusion, respectively, of transport vesicles with target membranes. The *G*olgi-*a*ssociated *r*etrograde *p*rotein (GARP) complex regulates retrograde transport from endosomes to the *trans*-Golgi network (TGN). Although GARP has been proposed to function as a tethering factor at the TGN, direct evidence for such a role is still lacking. Herein we report novel and specific interactions of the mammalian GARP complex with SNAREs that participate in endosome-to-TGN transport, namely, syntaxin 6, syntaxin 16, and Vamp4. These interactions depend on the N-terminal regions of Vps53 and Vps54 and the SNARE motif of the SNAREs. We show that GARP functions upstream of the SNAREs, regulating their localization and assembly into SNARE complexes. However, interactions of GARP with SNAREs are insufficient to promote retrograde transport, because deletion of the C-terminal region of Vps53 precludes GARP function without affecting GARP-SNARE interactions. Finally, we present in vitro data consistent with a tethering role for GARP, which is disrupted by deletion of the Vps53 C-terminal region. These findings indicate that GARP orchestrates retrograde transport from endosomes to the TGN by promoting vesicle tethering and assembly of SNARE complexes in consecutive, independent steps.**

Conveyance of cargo among organelles of the secretory and endosomal-lysosomal pathways is mediated by transport vesicles that bud from a donor compartment and fuse with an acceptor compartment in a specific and regulated manner (2, 25, 42). The accuracy and efficiency of vesicle fusion with the target compartment are provided by the concomitant actions of at least three protein families: tethers, small GTPases, and SNAREs. The general view is that a transport vesicle first finds its target organelle through interaction with tethering factors and then fuses with it through assembly of SNARE proteins while small GTPases of the Rab and Arl subfamilies orchestrate multiple steps of the overall process (1, 38, 44). The mechanistic details, however, are far from being completely understood and might vary depending on the transport pathway considered.

Tethering represents the first step in the interaction between a transport vesicle and its target membrane and results in the formation of physical links between two membranes that are bound to fuse. Two types of tethering factor, long coiled-coil proteins (e.g., p115, GCC185, and GM-130) and multisubunit complexes (e.g., HOPS/Vps-C, exocyst, COG, and GARP/VFT) have been implicated in nearly all vesicular transport routes (19, 38), although their direct role in connecting two opposing membranes has been documented for only a few (7, 40). Fusion is triggered by the assembly of SNAREs on the transport vesicle (v-SNAREs) with their cognate SNAREs on the target membranes (t-SNAREs) to form a SNARE pin or SNARE complex (12, 35). SNARE complex assembly involves the formation of a four-helix bundle that drives fusion of the two lipid bilayers (10, 14). Small GTPases participate in the initial recruitment of tethering factors and other peripherally associated effectors to specific locations on membranes, as well as in the subsequent fusion events (21). For example, the long coiled-coil protein GCC185 binds different GTPases, Rab9 on transport vesicles through the middle part and Rab6 and Arl1 at the *trans*-Golgi network (TGN) through the C-terminal part, thereby facilitating the recognition and connection of both membrane-bound compartments (11, 33). Other coiled-coil tethers have the ability to bind several different Rabs through domains that are not required for Golgi apparatus targeting. This supports a general model for a tentacular Golgi complex in which coiled-coil proteins capture and retain Rab-containing vesicles (33).

In addition to bringing together transport vesicles with target organelles, tethers may also regulate SNARE complex assembly, thus coordinating these two steps of vesicular transport. Several examples of tether-SNARE interactions have been reported, but no consensus for a mechanism of interaction or functional significance has yet emerged. For example, the HOPS complex associates with v- and t-SNARE complexes on *Saccharomyces cerevisiae* vacuoles both before and after fusion (37). Sec6p, a member of the exocyst complex, binds to the plasma membrane t-SNARE Sec9p, preventing its interaction with the cognate t-SNARE Sso1p (34). The COG complex binds the Golgi t-SNARE syntaxin 5 and enhances intra-Golgi SNARE complex stability (29). The long coiled-coil protein p115 also stimulates SNARE complex assembly (30).

The *G*olgi-*a*ssociated *r*etrograde *p*rotein (GARP) complex, also named the *V*ps *f*ifty-*t*hree (VFT) complex, together with COG and the exocyst, belongs to the quatrefoil family of mul-

* Corresponding author. Mailing address: Cell Biology and Metabolism Program, NICHD, Building 18T/Room 101, NIH, Bethesda, MD 20892. Phone: (301) 496-6368. Fax: (301) 402-0078. E-mail: juan@helix.nih.gov.

▽ Published ahead of print on 20 July 2009.

tisubunit tethering complexes (43), a structurally diverse group of peripheral membrane protein assemblies. Defects in the GARP, COG, or exocyst complexes cause accumulation of untethered vesicles that are scattered throughout the cytoplasm and contain different cargo proteins (18, 20, 45, 47). Direct proof of a tethering function for the GARP complex is still lacking, although its inactivation leads to defects consistent with a prominent role in the fusion of endosome-derived transport intermediates with the TGN (4–6, 20, 31). The yeast GARP complex is composed of four subunits named Vps51p, Vps52p, Vps53p, and Vps54p. Mutations in any of these subunits impair the retrieval of the secretory vesicle v-SNARE Snc1p and the carboxypeptidase Y receptor, Vps10p, from endosomes (5, 23, 32). The mammalian GARP complex also comprises Vps52, Vps53, and Vps54 subunits, but no Vps51 subunit has been identified to date (13). Depletion of the mammalian GARP complex prevents the delivery of Shiga toxin B subunit and the retrieval of TGN-localized proteins, such as TGN46, from endosomes to the TGN (20). Moreover, GARP depletion blocks the recycling of the cation-independent mannose 6-phosphate receptor (CI-MPR) from endosomes to the TGN, leading to missorting of the CI-MPR cargo, lysosomal hydrolases, into the extracellular space (20). The essential nature of mammalian GARP function in endosome-to-TGN transport is highlighted by the embryonic lethality of mice with ablation of the Vps54 subunit gene (27) and the motor neuron degeneration of Wobbler mice bearing a Vps54 hypomorphic mutation (27).

In yeast, the GARP subunit Vps51p specifically binds to the conserved N-terminal regulatory domain of the t-SNARE Tlg1p (5, 32). This finding led to the proposal that GARP tethers endosome-derived vesicles through its interaction with Tlg1p. However, deletions or point mutations that eliminate the binding of Vps51p to Tlg1p do not show any functional phenotype in vivo (8). Binding of Tlg1p to Vps51p is thus not essential for GARP-mediated vesicle tethering. In this work, we set out to study the possible link between the mammalian GARP complex and SNAREs. We found that GARP specifically and directly interacts with SNAREs that participate in the endosome-to-TGN retrograde route (i.e., syntaxin 6 [Stx6], Stx16, and Vamp4). These interactions depend on the fusion-inducing SNARE "motif" of the SNAREs and the N-terminal regions of Vps53 and Vps54. Functional analyses place the GARP complex upstream of the SNAREs, regulating their localization and assembly into SNARE complexes. In addition, we demonstrate that the GARP complex has a vesicle tethering function independent of its interaction with the SNAREs.

## MATERIALS AND METHODS

**Antibodies and other reagents.** The following antibodies were used as follows: immunofluorescence, immunoprecipitation, and/or immunoblotting: mouse monoclonal antibodies to the V5 epitope (Invitrogen, Carlsbad, CA), FLAG epitope (Sigma-Aldrich, St. Louis, MO), Vti1a and GM130 (BD Biosciences, San Diego, CA), rabbit polyclonal antibodies to human Vps52, Vps53, and Vps54 (20), p230 (46), green fluorescent protein (GFP; Invitrogen), Rab7 (Santa Cruz Biotechnology, Santa Cruz, CA), Stx6, Stx16, Vti1a, and Vamp4 (Synaptic Systems, Goettingen, Germany), sheep polyclonal antibody to human TGN46 (Serotec, Raleigh, NC), Alexa 488-, 594-, or -647-conjugated donkey anti-mouse immunoglobulin G (IgG), Alexa 488- or 594-, or 647-conjugated donkey anti-rabbit IgG, and Alexa 488- or 594-, or 647-conjugated donkey anti-sheep IgG (Molecular Probes, Eugene, OR), horseradish peroxidase (HRP)-conjugated donkey anti-mouse and donkey anti-rabbit IgG (Amersham Biosciences, Piscataway, NJ), and rabbit True-Blot HRP-conjugated anti-rabbit IgG (eBioscience, San Diego, CA).

Other reagents used included Strep-Tactin–Sepharose (IBA, St. Louis, MO), glutathione-Sepharose and protein A-Sepharose (GE Healthcare, Uppsala, Sweden), True-Blot anti-rabbit Ig immunoprecipitation (IP) beads (eBioscience), and Lipofectamine 2000 and Oligofectamine (Invitrogen). Chemicals were from Sigma-Aldrich.

**Recombinant DNA procedures.** Glutathione S-transferase (GST)-tagged constructs were generated by subcloning the cDNA for the cytosolic domains of the following human or mouse SNAREs into pGEX-5X-1 (GE Healthcare): human Stx8 1-216, Stx6 1-237, and Stx16 1-302 and mouse Stx7 1-236, Vamp4 1-114, Vti1a 1-192, and Vamp3 1-84 (residue numbers in each domain are indicated). All constructs were inserted into BamHI-XhoI or BamHI-NotI restriction sites. One-Strep-Flag(OSF)-Vps54 and OSF-Vps53 were generated by subcloning the respective human cDNAs into the KpnI-XhoI sites of pCAG-OSF (17), kindly provided by W. Sundquist (University of Utah, Salt Lake City). Introduction of a stop codon after residue 624 by site-directed mutagenesis generated OSF-Vps53 1-624. Human Vps53 and Vps52 were also cloned into NotI-BamHI or XhoI-BamHI sites, respectively, of pcDNA-FOS (17), kindly provided by W. Sundquist (University of Utah, Salt Lake City). Vps52-V5, Vps53-V5, and Vps54-V5 (20) and Vamp4-GFP (39) cDNAs have been previously described. GARP deletion mutants were cloned in frame with the V5 tag at their C termini in TOPO pEF6-V5-His (Invitrogen). Finally, human Vps53 (1-670; Δ57-95) was amplified by PCR from a total brain cDNA library. One of the isoforms cloned into TOPO pEF6-V5-His lacked an entire exon, leading to the deletion of residues 57 to 95.

**In vitro binding assays.** GST-tagged proteins were expressed in *Escherichia coli* BL21 cells after isopropyl-β-D-thiogalactopyranoside (IPTG) induction and affinity purified on glutathione-Sepharose beads (GE Healthcare) from 50-ml or 500-ml cultures. Protein concentration was estimated by sodium dodecyl sulfate-polyacrylamide gel electrophoresis (SDS-PAGE) and Coomassie blue staining of aliquots taken from washed beads. When needed, GST-protein fusions were eluted in elution buffer (50 mM Tris-HCl, pH 8.0, 100 mM NaCl, 20 mM glutathione). SNARE complexes were formed by incubating soluble proteins (~250 μg each) on ice for 48 to 72 h in elution buffer. Complexes were separated from individual SNAREs by gel filtration, using a Hi Load 16/60 Superdex 200 column (GE Healthcare) equilibrated in 50 mM Tris-HCl, pH 8.0, 100 mM NaCl, 1 mM dithiothreitol (DTT) buffer. For in vitro binding assays, typically 20 μg of GST-tagged proteins in 10 to 25 μl of glutathione-Sepharose beads was mixed with total clarified cell extracts (500 μg protein) in lysis buffer (50 mM Tris-HCl, pH 7.5, 150 mM NaCl, 10% glycerol, 5 mM EDTA, 0.5% [vol/vol] NP-40, and a protease inhibitor cocktail [Roche Applied Science, Indianapolis, IN]) supplemented with 1 mg of bovine serum albumin (BSA) and incubated at 4°C for 18 h. After extensive washing, GST-tagged and coprecipitated proteins were eluted in sample buffer and separated by SDS-PAGE, and interactions were determined by immunoblotting.

For the purification of recombinant GARP complex, six 100-mm dishes containing HeLa cells were transiently transfected with cDNAs encoding OSF-Vps54 (which incorporates a One-Strep-Flag epitope tag at the N terminus of the protein), Vps53, and Vps52. Proteins were extracted in lysis buffer and microcentrifuged, and the GARP complex was isolated by affinity purification with Strep-Tactin–Sepharose beads. Bound proteins were eluted in buffer containing 2 mM biotin, followed by ultracentrifugation at 100,000 × *g* for 10 min to remove protein aggregates. One-tenth of the purified complex material was typically used for in vitro binding to GST-SNAREs as described above.

**Cell transfection and immunoprecipitation.** Human HeLa epithelial cells (American Type Culture Collection, Manassas, VA) were cultured on 24-well plates or 100-mm dishes at 37°C in Dulbecco's modified Eagle's medium (Invitrogen) with high glucose and supplemented with 10% (vol/vol) fetal bovine serum (FBS), 100 U/ml penicillin, and 100 μg/ml streptomycin. When cells reached 40 to 80% confluence, they were transfected with 0.8 to 10 μg plasmids using Lipofectamine 2000 (Invitrogen). For immunoprecipitation experiments, cells were extracted in lysis buffer on ice for 30 min and microcentrifuged. Lysates were further clarified with 30 μl protein A-Sepharose beads (Amersham Biosciences) before adding specific antibodies (2 μl sera) bound to protein A-Sepharose beads and rocking at 4°C for 16 h. Immunoprecipitated material was washed four times in phosphate-buffered saline (PBS) and eluted from the beads by heating at 90°C for 3 min in Laemmli sample buffer. Samples were subsequently analyzed by SDS-PAGE and immunoblotting.

For immunoprecipitation of SNARE complexes, a modified protocol was used as described in reference 15 in order to freeze newly formed SNARE complexes. Briefly, control, GARP-depleted, or Rab7-depleted cells grown on six-well plates were incubated in medium containing 1 mM *N*-ethylmaleimide (NEM) for 15

min on ice, washed, and further incubated in medium supplemented with 2 mM DTT for 15 min on ice. Cells were finally incubated in complete medium at 37°C for 30 min before extraction in lysis buffer. Polyclonal antibodies directed to different SNARE proteins were prebound to True-Blot anti-rabbit Ig IP beads (eBioscience; 2 μl sera in 30 μl of beads per IP mixture). Cell lysates (350 μg protein) diluted in 700 μl of lysis buffer were supplemented with 1 mg BSA and incubated with the True-Blot beads containing the corresponding antibodies at 4°C for 16 h. Immunoprecipitated material was analyzed as above but we employed HRP-conjugated secondary antibodies compatible with the True-Blot system.

**Immunofluorescence microscopy and Vamp4-GFP internalization assays.** Immunofluorescence microscopy was performed as described previously (20). Antibody uptake assays were carried out by incubation for 40 min at 37°C of HeLa cells grown on coverslips in the presence of polyclonal antibody to GFP diluted 1:100 in Dulbecco's modified Eagle's medium, 1% BSA, and 25 mM HEPES, pH 7.4. The cells were washed in PBS, chased in complete medium for 40 min, washed again in PBS, and fixed in −20°C methanol.

**In vitro tethering assays.** Recombinant GARP complex was purified basically as described above using Strep-Tactin–Sepharose beads. Different combinations of OSF-tagged GARP subunits were used as follows: OSF-Vps54/Vps53/Vps52, Vps54/OSF-Vps53/Vps52, or Vps54/OSF-Vps53 (1-624)/Vps52. Between one and eight 100-mm dishes containing transiently transfected HeLa cells were used per experiment. GARP bound to Strep-Tactin–Sepharose was used as the solid phase.

For the isolation of vesicles containing retrograde cargo, two 100-mm dishes containing HeLa cells depleted of Vps52 were transfected with Vamp4-GFP cDNA for 24 h. Cells were collected and postnuclear supernatants were prepared in hypotonic buffer and fractionated on glycerol 10 to 30% gradients as described previously (20). Fractions 4 to 6, containing vesicles and transport intermediates enriched for retrograde cargo and Vamp4-GFP, were pooled, diluted in an equal volume of 2× tethering buffer (25 mM HEPES, pH 7.0, 2.5 mM magnesium acetate, 100 mM KCl, 1 mM DTT, and 9% sucrose), and incubated with immobilized GARP for 18 h at 4°C. Beads were washed twice in tethering buffer and eluted in sample buffer. Similar incubation with Strep-Tactin beads previously incubated with lysates of untransfected cells was performed as a control. Binding of retrograde vesicles was monitored through detection of Vamp4-GFP by immunoblotting.

**Quantification and statistical analyses.** For the quantification of immunoblots, chemiluminescence signals were recorded on a Typhoon 9200 PhosphorImager (Amersham Biosciences) whenever the signal intensity was strong enough and later analyzed using ImageQuant analysis software (Molecular Dynamics). Alternatively, blots were exposed to BioMax XAR films (Kodak) and the lowest consistent exposures were scanned and quantified using ImageQuant software. For the analysis of SNARE complex formation in vivo, the densitometry data of coimmunoprecipitated proteins were normalized to the efficiency of the primary immunoprecipitation and the starting levels of the analyzed SNARE present in the lysates, when these were lower for GARP-depleted cells. Student's *t* test analysis of paired data was performed to assess the significance of coimmunoprecipitation results.

**Other methods.** Electrophoresis, immunoblotting, site-directed mutagenesis, small intefering RNA (siRNA) treatments, and glycerol gradient subcellular fractionation analysis were all performed as previously described (20, 24).

## RESULTS

**Interaction of GARP with SNAREs involved in transport from endosomes to the TGN.** Because the mammalian GARP complex functions in retrograde transport from endosomes to the TGN (20), we tested for interactions of GARP with SNAREs that play a role in this pathway. In particular, we focused on a SNARE complex composed of the t-SNAREs Stx6, Stx16, and Vti1a and the v-SNARE Vamp4, which is required for the retrograde transport of the same cargoes that are dependent on GARP (15). These SNAREs are cytosolically disposed proteins anchored to the membrane by a C-terminal transmembrane domain (12). The complete cytosolic portions of these SNAREs and of the closely related Stx7, Stx8, and Vamp3 were expressed as GST-fusion proteins, immobilized on glutathione-Sepharose, and used in pull-down assays of GARP binding. To facilitate analyses of GARP-SNARE interactions and given the absence of proper antibodies to all GARP subunits, we performed the pull-down assays with detergent extracts of HeLa cells expressing the three mammalian GARP subunits tagged with the V5 epitope (Vps52-V5, Vps53-V5, and Vps54-V5). These recombinant proteins were expressed at levels that were slightly higher than those of the endogenous proteins and were assembled into a mixture of partial and whole GARP complexes, as previously described (20). We observed that the three epitope-tagged GARP subunits were efficiently pulled down, in a concentration-dependent manner, by GST-Stx6, -Stx16, and -Vamp4 but not -Stx7, -Stx8, or -Vamp3 (Fig. 1A and B; notice in the Ponceau staining the large excess of GST-Stx7 and GST-Stx8 used in this experiment). The amount of recombinant GARP pulled down by GST-Stx6, -Stx16, and -Vamp4 was usually >10% of the input, a fraction that was larger than that of the endogenous cognate t-SNARE Vti1a pulled down by the same GST-SNAREs (Fig. 1A). In contrast, GST-Vti1a pulled down only a small amount of recombinant GARP subunits (Fig. 1B).

**Delineation of protein domains involved in GARP-SNARE interactions.** Next, we used the pulldown assay with epitope-tagged GARP subunits to determine the domains involved in the interactions. Syntaxins consist of a regulatory N-terminal trihelical bundle called the Habc domain, a flexible linker region, a coiled-coil SNARE motif, and a C-terminal transmembrane anchor (Fig. 2A). Vamp4 comprises a shorter regulatory N-terminal domain that contains sorting information, a coiled-coil SNARE motif, and a C-terminal transmembrane anchor (Fig. 2A). Dissection of the SNAREs showed that the SNARE motifs from Stx16 (residues 245 to 302), Stx6 (residues 176 to 236) and Vamp4 (residues 50 to 114) bound V5-tagged GARP subunits with efficiencies that were similar to those of the full-length cytosolic domains (Fig. 2B). In addition, Stx6 1-176, which contains the Habc domain, also bound the GARP subunits (Fig. 2B).

To identify the GARP subunit counterparts for these interactions, we expressed different combinations of V5-tagged GARP subunits by transient transfection into HeLa cells and incubated the corresponding lysates with GST-SNARE proteins. We found that a combination of Vps53 and Vps54 was pulled down as efficiently as the trimeric GARP complex by GST-Stx6, -Stx16, and -Vamp4 (Fig. 2C). Other combinations, as well as single GARP subunits, showed much less interaction with all the GST-SNAREs tested (Fig. 2C). This probably reflects a requirement of both Vps53 and Vps54 subunits for folding or a SNARE binding site that spans the surface of both subunits. The N-terminal halves of Vps53 and Vps54 are predicted to contain α-helical coiled-coils, as is the case for subunits of other quatrefoil tethering complexes, such as COG or the exocyst (44). We found that these N-terminal regions of Vps53 (residues 1 to 624) and Vps54 (residues 1 to 442) were responsible for the interaction with GST-Vamp4 (Fig. 2D) as well as GST fused to the SNARE motifs of Stx6 and Stx16 (data not shown). We also found that deletion of residues 57 to 95 from Vps53, comprising a predicted coiled-coil (residues 54 to 82), prevented both assembly with Vps54 and binding to GST-Vamp4 (Fig. 2D). Although this deletion could interfere with proper protein folding and stability, this coiled-coil region most likely interacts with Vps54, since antibodies directed toward this domain pull down Vps53 but not Vps54, unlike

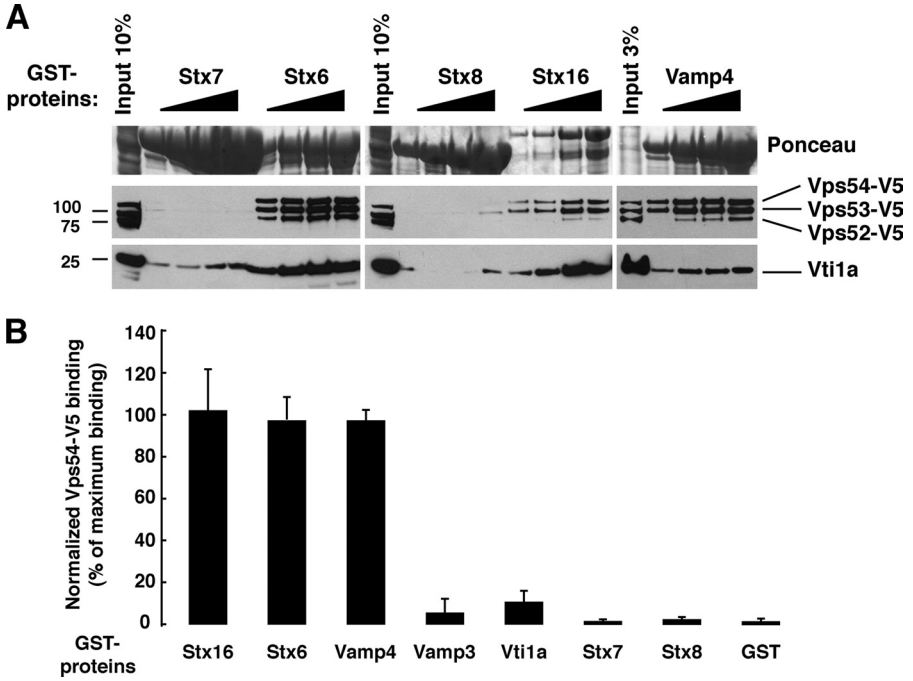


FIG. 1. The GARP complex specifically interacts with SNAREs involved in endosome-to-TGN transport. (A) In vitro binding assay of GARP to the cytosolic portions of different SNAREs. Serial dilutions of a glutathione-Sepharose bead slurry with prebound GST-SNAREs (0.1 to 100 μg) were incubated with detergent lysates from HeLa cells (500 μg of protein) transiently transfected with plasmids encoding Vps54, Vps53, and Vps52, all tagged with the V5 epitope. Bound proteins were analyzed by immunoblotting with antibodies to the V5 epitope and to Vti1a. Blots were also stained with Ponceau Red to estimate the amounts of GST-protein fusions. Samples of the total lysates (10% or 3%) were included as input controls. (B) The results from at least four independent experiments were quantified and plotted in a bar graph as the percentage of V5-tagged Vps54 binding normalized to the amount of GST-SNARE. Maximum V5-tagged Vps54 binding was set at 100% for each independent experiment. Bars represent the means and error bars represent standard deviations.

antibodies directed to Vps54, which recover both Vps53 and Vps54 (20).

**GARP-SNARE interactions are direct.** Because the pull-down assays were performed using cell lysates as the source of V5-tagged GARP proteins, the observed interactions could have been indirect. To test for direct interactions, we purified recombinant trimeric GARP complex using the Strep-tag system (26). To this end, an OSF tag was placed at the N terminus of Vps54, and this construct was coexpressed with untagged Vps52 and Vps53 by transfection into HeLa cells. The trimeric complex was affinity purified with Strep-Tactin–Sepharose beads and eluted in the presence of biotin. Purified recombinant OSF-Vps54 was visible by silver staining, together with two extra bands corresponding to Vps53 and Vps52 (Fig. 3A). Pull-down experiments demonstrated specific binding of this recombinant complex to GST-Stx6, - Stx16, and -Vamp4, with only background binding to GST alone or GST-Stx7 (Fig. 3B), as happened with total cell lysates (Fig. 1). These results demonstrated that GARP-SNARE interactions are direct and specific.

**Interaction of GARP with assembled SNARE complexes.** SNAREs exert their actions by assembling four different SNARE motifs into a four-helix bundle to form a SNARE complex (12). Since GARP binds to the SNARE motif, we asked whether SNARE complex formation affects GARP binding. To address this question, SNARE complexes composed of GST fused to Stx16, Vamp4, Vti1a, and the SNARE motif of Stx6 (residues 176 to 236) were assembled in vitro and separated from unassembled proteins by gel filtration (Fig. 3C, fractions 5 and 6). The Habc domain of Stx6 was intentionally deleted to remove a second binding site for GARP, which could complicate interpretation of the results. Pull-down experiments using V5-tagged GARP subunits expressed by transfection in HeLa cells showed that these proteins bound to the assembled SNARE complex (4xSNARE) just as well as the individual SNAREs (Fig. 3D). From these experiments, we concluded that the GARP complex can bind both to single SNAREs and to assembled SNARE complexes.

**Coprecipitation and colocalization of GARP with TGN SNAREs.** To verify that the GARP-SNARE interactions detected in vitro can also occur within cells, we examined the coprecipitation of endogenous SNAREs with V5-tagged GARP subunits expressed by transfection in HeLa cells (Fig. 4). We observed that a small, but consistent, amount of GARP coprecipitated with the SNAREs using antibodies to Stx6, Stx16, and Vamp4, but not with a control antibody (Fig. 4A). Immunofluorescence microscopy showed that V5-tagged Vps54 colocalized with endogenous Stx16 as well as with GFP-tagged Vamp4 (39) at the TGN (Fig. 4B). In addition, we found that endogenous Stx6 localized to both the TGN and more peripheral structures and that the TGN population colocalized with V5-tagged Vps54 (Fig. 4B). Therefore, GARP-SNARE interactions likely occur at the TGN.

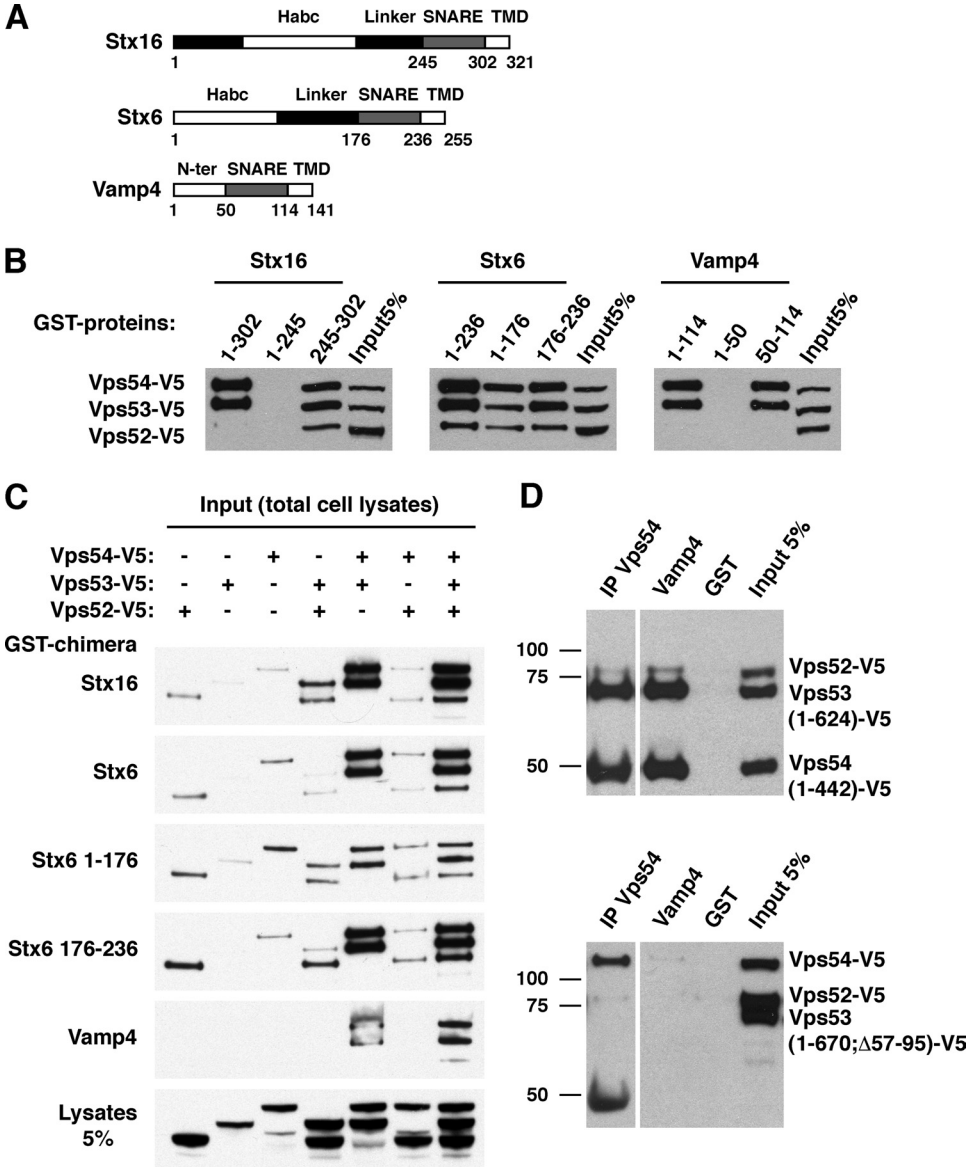


FIG. 2. The GARP complex interacts with the SNARE motif of TGN SNAREs through a Vps53-Vps54 dimer. (A) Schematic representation of the domain organization of Stx16, Stx6, and Vamp4. Amino acid residue numbers are indicated. (B) The whole cytosolic domains, N-terminal regulatory domains, or SNARE motifs of Stx16, Stx6, and Vamp4 fused to GST (20 μg each, except for Stx16 1-302, for which 10 μg was used) were incubated with HeLa cell detergent lysates expressing Vps52, Vps53, and Vps54, all tagged with the V5 epitope, as described in the legend for Fig. 1. (C) The cytosolic domains of Stx16, Stx6, or Vamp4 (10 μg each), or Stx6 1-176 or Stx6 176-236 (20 μg each), fused to GST, were incubated with detergent lysates from HeLa cells transfected with the combinations of V5-tagged GARP subunit cDNAs indicated on the top of the figure. (D) GST fused to Vamp4 or GST alone (20 μg each) was incubated with detergent lysates from HeLa cells expressing V5-tagged versions of Vps52 and the N-terminal domains of Vps54 Vps54(1-442) and Vps53 Vps53(1-624) (upper panel) or Vps52, Vps54, and a Vps53 mutant with an internal deletion, Vps53(1-670;Δ57-95) (lower panel). The same detergent lysates were subjected to IP with antibodies directed to Vps54. Pulled-down and immunoprecipitated proteins were identified by immunoblotting with antibody to the V5 epitope. The positions of molecular mass markers (in kDa) are indicated on the left.

**Decreased SNARE complex formation in cells depleted of GARP.** Given the physical interaction and colocalization of GARP with TGN SNAREs, we asked whether GARP might regulate the formation of SNARE complexes in vivo. To address this question, we performed native immunoprecipitation of TGN SNAREs in control and GARP-depleted cells. In order to stabilize SNARE complexes, cells were treated with NEM to inhibit NSF and thus prevent SNARE disassembly. Immunoprecipitation of Vti1a revealed a significant decrease (two to threefold; $P < 0.01$) in the coisolation of both Vamp4 and Stx16 in Vps54-depleted cells (Fig. 5A and B). Likewise, immunoprecipitation of Vamp4 recovered significantly lower amounts of Vti1a and Stx16 (twofold; $P < 0.05$), and Stx16 immunoprecipitation resulted in lower amounts of coprecipitated Vamp4 and Vti1a (two to threefold; $P < 0.001$) (Fig. 5A and B). Similar results were obtained after depletion of Vps52

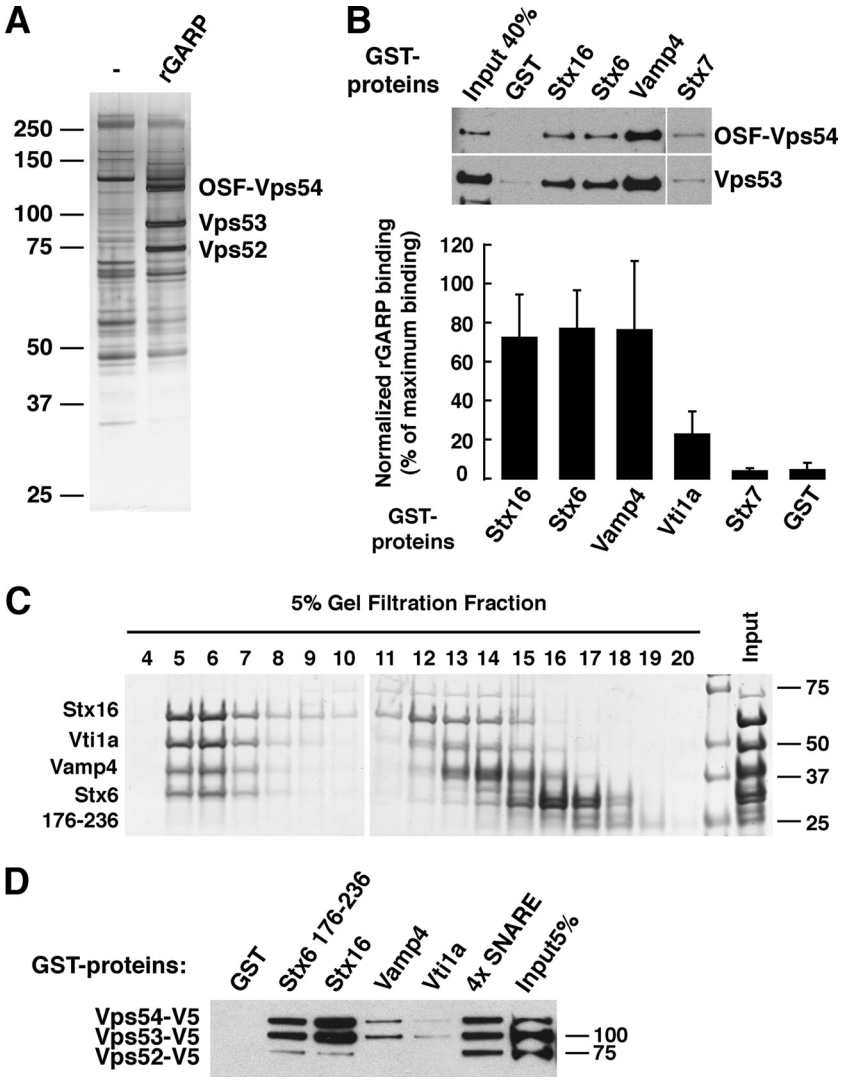


FIG. 3. GARP-SNARE interactions are direct and maintained in assembled SNARE complexes. (A) Purification of recombinant GARP complex on Strep-Tactin–Sepharose beads from one 100-mm dish of HeLa cells transiently transfected with OSF-Vps54, Vps53 and Vps52 cDNAs as described in Materials and Methods. Eluted proteins were separated by gel electrophoresis and visualized by silver staining. A sample derived from untransfected HeLa cells was used as a control for nonspecific binding to Strep-Tactin beads. The positions of molecular mass markers (in kDa) are indicated on the left. (B) Purified recombinant GARP specifically binds Stx6, Stx16, and Vamp4. Recombinant GARP was used in pull-down experiments with 20 μg of GST, GST-Vamp4 or -Stx7, or 7 μg of GST-Stx16 or -Stx6. Bound GARP was detected by immunoblotting with antibodies to Vps53 and to the FLAG epitope (contained within the OSF tag). GARP binding was measured by densitometry, normalized to the starting GST-SNARE amounts, and expressed as the percentage of maximum binding per experiment. The means ± standard deviations from three independent experiments are plotted in the lower panel. (C) Isolation of assembled TGN-SNARE complex. The four individual GST-SNAREs indicated in the figure (250 μg each) were incubated for 48 h at 4°C, and assembled complexes were purified by gel filtration. Aliquots of the fractions (5%) were separated by SDS-PAGE and stained with Coomassie blue. Fractions 5 and 6, containing assembled SNARE complexes, were rebound to glutathione-Sepharose beads. (D) TGN SNARE complex (4xSNARE) or the individual SNAREs (10 to 20 μg each) bound to glutathione-Sepharose beads were incubated with detergent lysates of HeLa cells transfected with V5-tagged GARP subunit cDNAs, as described for Fig. 1. Data shown are representative of three experiments with similar results.

or Vps53 (data not shown), indicating that the formation of the TGN-specific Stx16-containing SNARE complex is partially prevented by the absence of GARP.

**Redistribution of TGN SNAREs in cells depleted of GARP.** The GARP dependence of SNARE complex assembly could result from a direct effect on assembly or from a requirement for proper localization of the SNAREs to sites of assembly. To assess this latter possibility, we examined the localization of TGN SNAREs after GARP depletion. Sedimentation velocity analysis of postnuclear supernatants from Vps52-depleted cells on glycerol gradients showed a shift of Stx16, Vamp4, and Vti1a to light membrane fractions (Fig. 6A, fractions 5 to 7) previously shown to represent intermediates in retrograde transport from endosomes to the TGN (20). In addition, immunofluorescence microscopy showed partial loss of Stx16 and TGN46 staining at the TGN in Vps52-depleted cells (Fig. 6B). To determine whether depletion of GARP inhibited retrograde transport of SNAREs to the TGN, we followed the

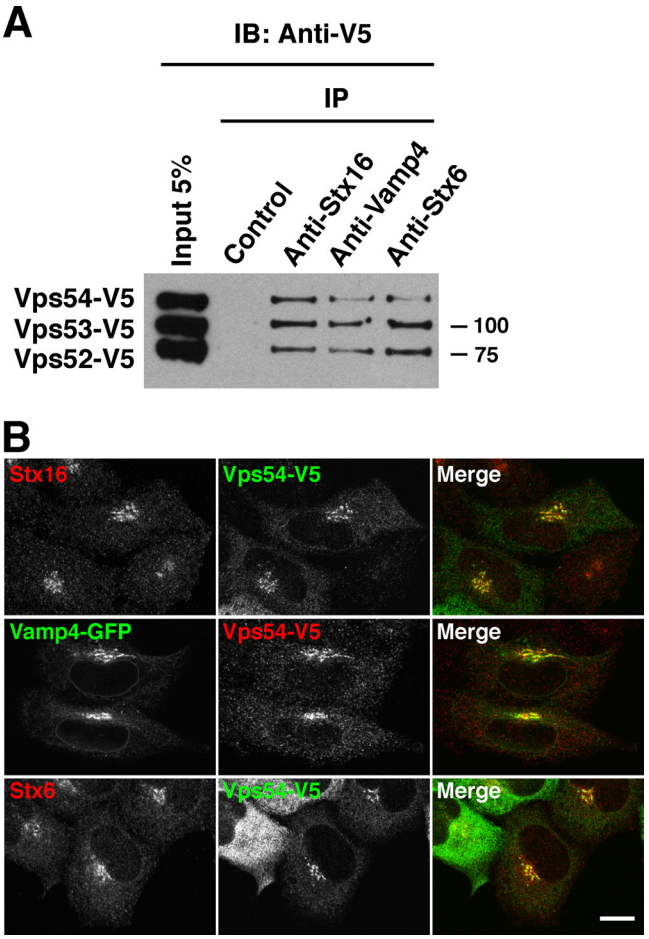


FIG. 4. The GARP complex interacts and colocalizes with TGN SNAREs in vivo. (A) Detergent lysates from HeLa cells expressing V5-tagged GARP subunits were immunoprecipitated with antibodies to Stx16, Vamp4, or Stx6 or with a control preimmune serum. IP were separated by SDS-PAGE, and GARP subunits were detected by immunoblotting (IB) with antibody to the V5 epitope. (B) HeLa cells grown on glass coverslips were transiently transfected with V5-tagged Vps54 (first and third rows) or with V5-tagged Vps54 and GFP-tagged Vamp4 (second row) cDNAs. Twenty-four hours later, cells were fixed in −20°C methanol, labeled with antibodies to the indicated proteins followed by secondary antibodies, and analyzed by confocal fluorescence microscopy. Yellow in the merged images indicates colocalization. Bars, 10 μm.

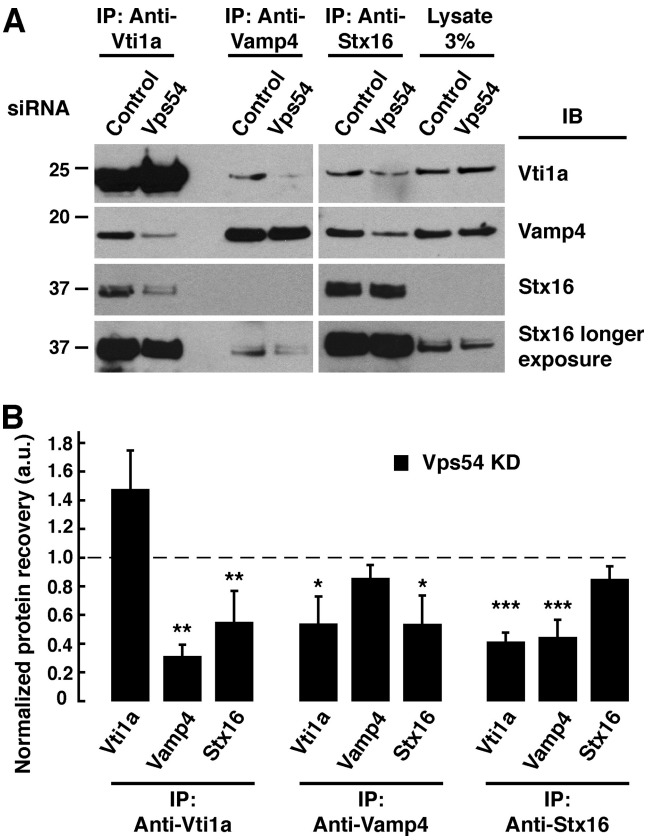


FIG. 5. TGN SNARE complex formation is reduced in GARP-depleted cells. (A) TGN SNARE complex formation analyzed by coimmunoprecipitation. HeLa cells were transfected twice at 72-h intervals with siRNA directed toward Vps54 or without siRNA (control). Seventy-two hours after the second transfection, cells were treated with NEM to stabilize SNARE complexes, as described in Materials and Methods. SNARE complexes were isolated by IP from cell lysates with the antibodies indicated on top of the panel, employing the TrueBlot system to eliminate interference by the heavy and light chains of the immunoprecipitating antibodies. Proteins in the immunoprecipitates, along with 3% of the total input lysate, were separated by SDS-PAGE and analyzed by immunoblotting (IB) with antibodies to endogenous TGN SNAREs. Results from three to seven independent experiments were quantified, normalized to the efficiencies of immunoprecipitations and the starting levels of SNAREs, and plotted as protein recovered relative to the control condition (no siRNA treatment; indicated by the dash line). Means ± standard deviations are shown in (B). *P* values are as follows: *, $P < 0.05$; **, $P < 0.01$; ***, $P < 0.001$.

internalization of antibody to GFP in cells expressing Vamp4 appended with a luminal/extracellular GFP tag (39). After 40 min of antibody uptake and 40 min of chase, the majority of internalized anti-GFP was found in the TGN area, colocalizing with TGN46 and with total Vamp4-GFP, in control cells (Fig. 6C). In contrast, in GARP-depleted cells internalized Vamp4-GFP localized mostly to peripheral vesicles characteristic of endosomes, clearly distinct from a fraction of the total Vamp4-GFP pool, which was more concentrated in the TGN area (Fig. 6C). Therefore, retrieval of Vamp4-GFP from endosomes to the TGN is impaired in GARP-depleted cells. From these results, we concluded that decreased assembly of TGN SNARE complexes in the absence of GARP might be due in part to mislocalization of the SNAREs. Because the mislocalized SNAREs are present in the same subcellular fractions (Fig. 6A), however, a direct effect of GARP on SNARE complex assembly also appears likely. In support of this latter interpretation, Rab7-depleted cells also exhibited a partial block in the retrieval of Vamp4-GFP from the plasma membrane to the TGN (Fig. 7A) but no defect in SNARE complex formation (Fig. 7C). Therefore, SNARE redistribution is not likely the cause for the decreased SNARE complex formation in GARP-depleted cells.

**The ability of GARP to interact with SNAREs is insufficient to support retrograde transport to the TGN.** To determine if GARP has functions other than promoting SNARE complex assembly, we tested the effect of overexpressing the N-terminal Vps53 1-624 and Vps54 1-442 fragments, which can assemble

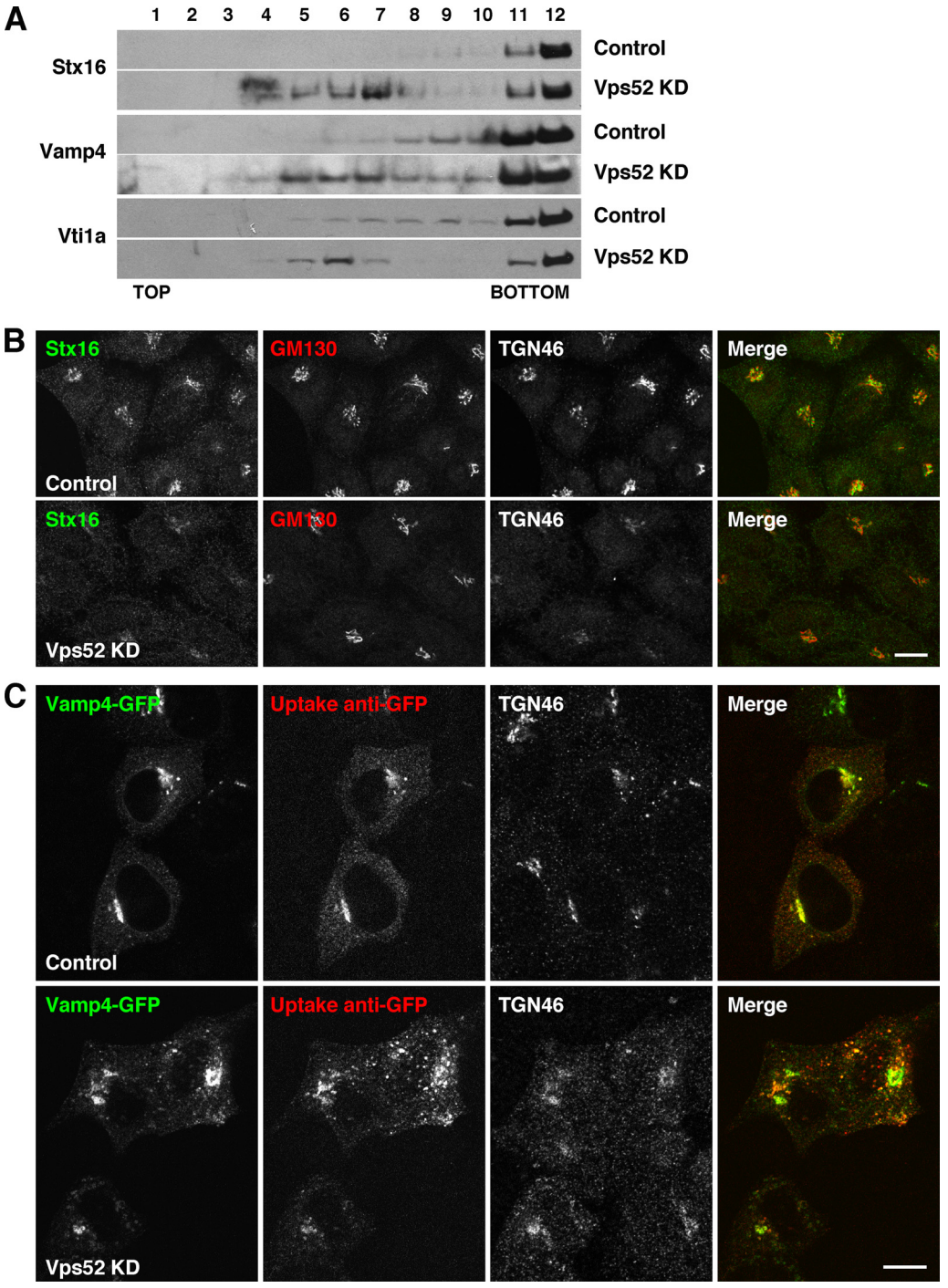


FIG. 6. GARP depletion results in redistribution of TGN SNAREs and inhibition of Vamp4-GFP retrograde trafficking to the TGN. (A) Subcellular fractionation by sedimentation velocity on glycerol gradients shows that TGN SNARE proteins accumulate in a light membrane fraction in Vps52-depleted cells. HeLa cells were transfected twice at 24-h intervals with siRNA directed to Vps52 (Vps52 KD) or without siRNA (control). Postnuclear supernatants from both cell types were prepared 48 h after the second round of transfection, loaded on top of a 10 to 30% glycerol gradient, and analyzed by sedimentation velocity. The distribution of Stx16, Vamp4, and Vti1a was determined by immunoblotting of gradient fractions with specific antibodies. (B) Vps52 depletion results in redistribution of Stx16. HeLa cells were transfected with siRNA directed to Vps52 (KD) or without siRNA (control) and analyzed by confocal immunofluorescence microscopy 72 h later. Cells were fixed in methanol and labeled with antibodies to the indicated proteins followed by appropriate secondary antibodies. (C) Defective retrograde trafficking of internalized Vamp4-GFP in GARP-depleted cells. Control cells or cells depleted of Vps52 for 72 h were transfected with Vamp4-GFP cDNA for 24 h. Live cells were then incubated in the continuous presence of rabbit polyclonal antibody to GFP for 40 min at 37°C, washed, and chased for another 40 min in complete medium before fixation and analysis by immunofluorescence microscopy. The total Vamp4-GFP pool was monitored by the intrinsic GFP fluorescence, whereas internalized Vamp4-GFP was detected with secondary antibodies directed toward the internalized anti-GFP (notice the amplification of the fluorescence signal by the antibodies compared to the intrinsic fluorescence of Vamp4-GFP). Bars, 10 μm.

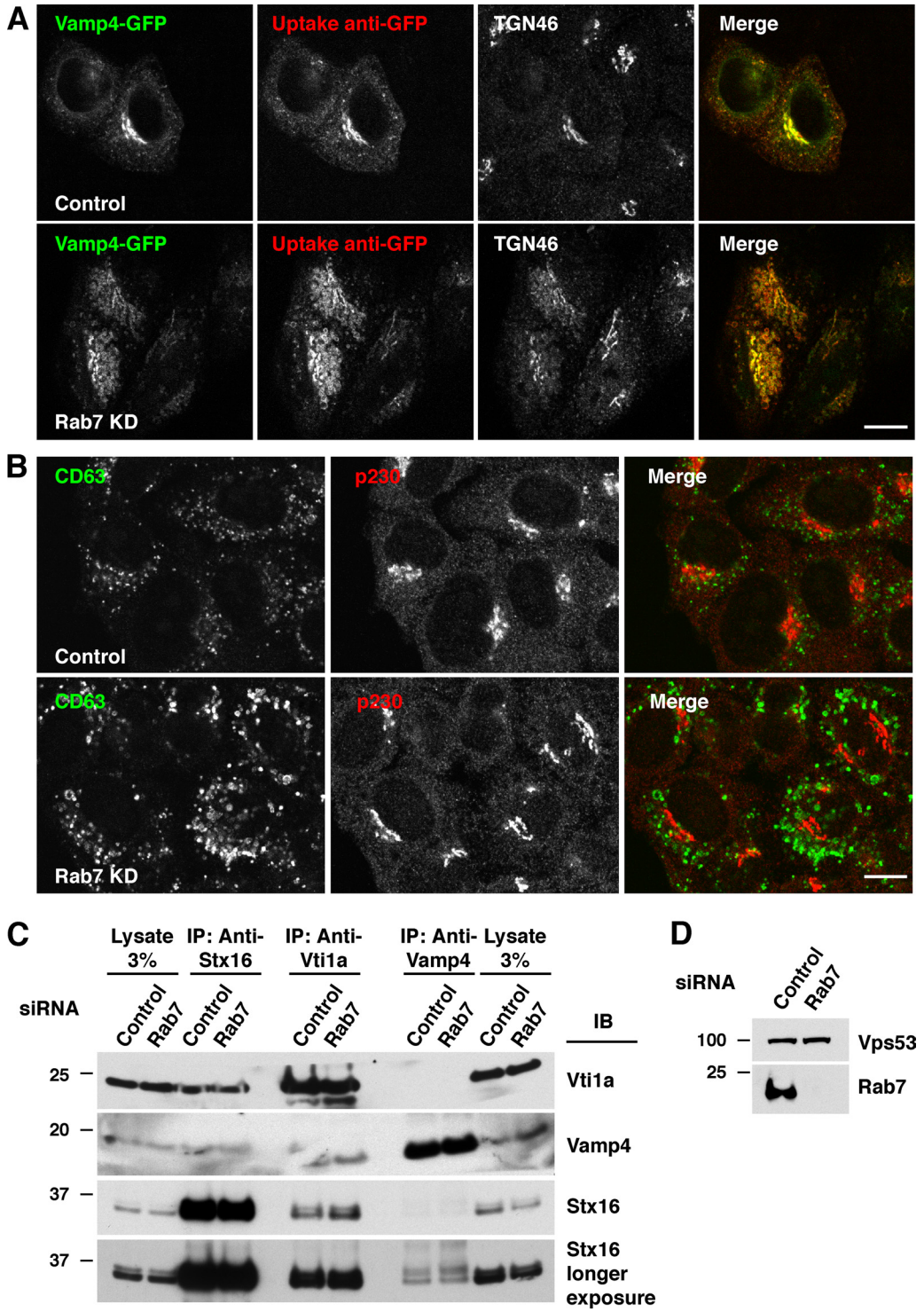


FIG. 7. Rab7 depletion affects retrograde traffic of Vamp4-GFP but not TGN SNARE complex formation. (A) Altered retrograde trafficking of internalized Vamp4-GFP in Rab7-depleted cells. HeLa control cells or cells depleted of Rab7 (two shots within 72 h) were transfected with Vamp4-GFP cDNA for 24 h. Live cells were then incubated in the continuous presence of rabbit polyclonal antibody to GFP for 40 min at 37°C, washed, and chased for another 40 min in complete medium before fixation and analysis by immunofluorescence microscopy as described for Fig. 6C. More than 60% of Rab7-depleted cells showed retention of Vamp4-GFP in endosomal-like compartments. (B) Rab7 depletion causes lysosomal swelling. HeLa cells were transfected twice within 48 h with siRNA directed to Rab7 (KD) or without siRNA (control) and analyzed by confocal immunofluorescence microscopy 48 h later. Cells were fixed in methanol and labeled with antibodies to the indicated proteins followed by appropriate secondary antibodies. Bars, 10 μm. (C) TGN SNARE complex formation analyzed by coimmunoprecipitation. HeLa cells were transfected twice at 48-h intervals with siRNA directed towards Rab7 or without siRNA (control). At 48 h after the second transfection, cells were treated with NEM to stabilize SNARE complexes as described in Materials and Methods. SNARE complexes were isolated by IP from cell lysates as indicated in Fig. 5. One representative experiment of two performed is shown. (D) Assesment of Rab7 depletion efficiency. Endogenous levels of Rab7 were analyzed by immunoblotting of the same protein lysates as those in panel C. Vps53 levels are also shown as a loading control.

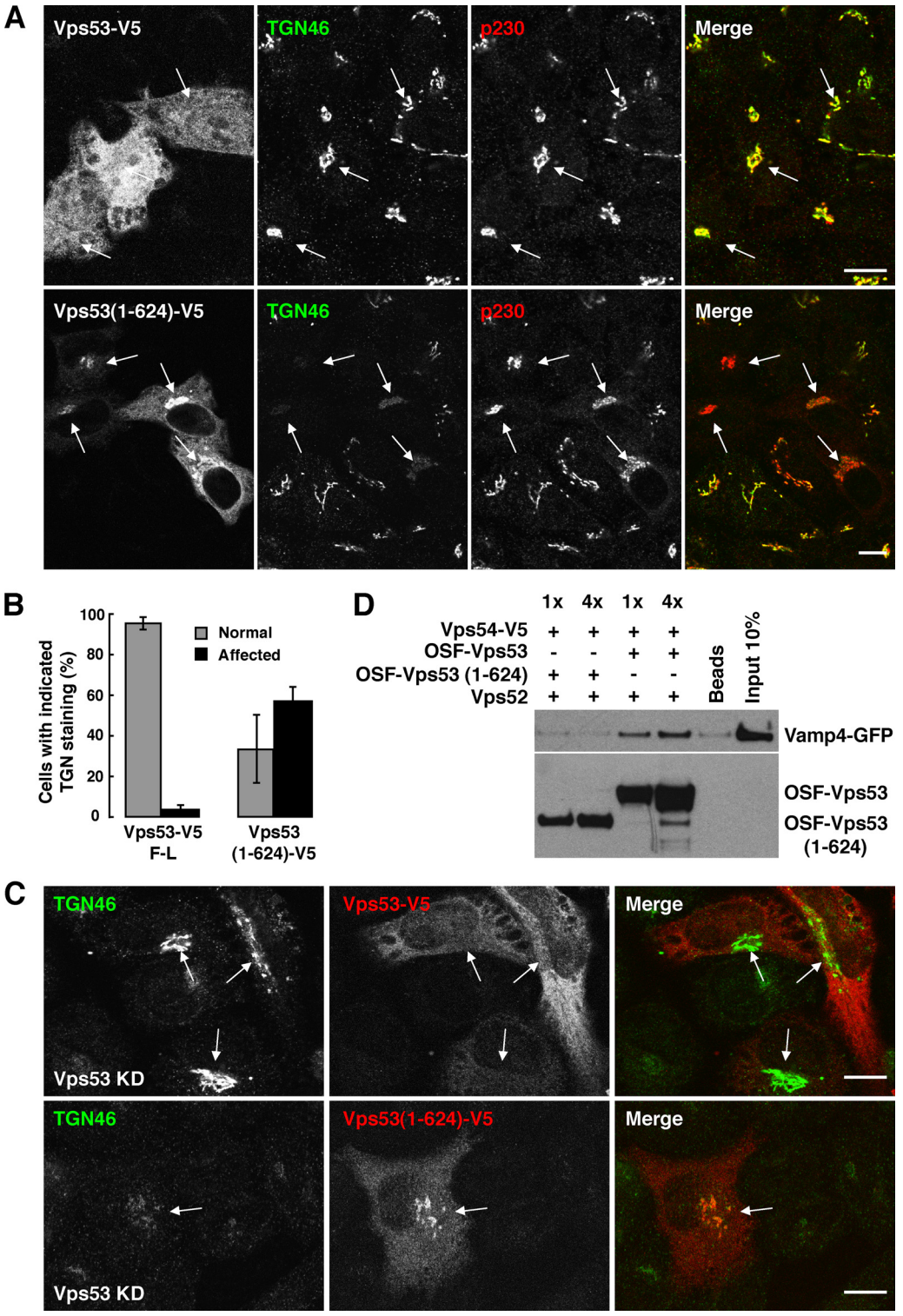


FIG. 8. Overexpression of the Vps53 SNARE-interacting domain affects retrograde trafficking to the TGN due to its inability to promote vesicle tethering. (A) HeLa cells were transfected with plasmids encoding V5-tagged Vps53 (top panels) or the deletion mutant Vps53(1-624) (bottom panels). Cells were fixed 48 h later, triple labeled with antibodies to the indicated proteins followed by secondary antibodies, and analyzed by confocal immunofluorescence microscopy. Notice that TGN46 is lost from the TGN in cells expressing the deletion mutant but not the full-length protein (arrows). (B) Results from three independent experiments ($n > 150$ cells for each condition) such as that in panel A were scored visually and plotted as the percentage of overexpressing cells showing either a typical TGN (normal TGN46 staining) or an acute decrease in the TGN46 signal at the TGN (affected TGN46 staining). (C) Vps53(1-624)-V5 is unable to rescue cells depleted of Vps53. HeLa cells were transfected twice at 24-h intervals with siRNA directed to Vps53. At 24 h after the second transfection, cells were seeded on coverslips and transfected the following day with plasmids encoding siRNA-resistant full-length V5-tagged Vps53 (top panels) or Vps53(1-624) (bottom panels) cDNAs. Cells were fixed

with other GARP subunits and interact with TGN SNAREs (Fig. 2D) but may be defective in other activities. As an indicator of GARP function we examined the localization of TGN46, a protein that recycles from endosomes to the TGN in a GARP-dependent manner (20). We observed that overexpression of truncated Vps53 1-624 decreased the TGN localization of TGN46 in 56% of the cells ($n = 300$), whereas overexpression of full-length Vps53 had the same effect in only 4% of the cells ($n = 150$) (Fig. 8A and B). Overexpression of Vps53 1-624 together with Vps54 1-442 gave similar results (data not shown). This dominant-negative effect indicated that the ability of Vps53 1-624 to assemble into the complex and interact with SNAREs (Fig. 2D) is insufficient to support TGN46 recycling to the TGN. The C-terminal part of Vps53 must therefore also be important for function.

We also tested the functional rescue of GARP-depleted phenotypes by different Vps53 constructs. To this end, cells depleted of Vps53 by RNA interference (RNAi) were transfected with RNAi-resistant forms of either full-length Vps53 or truncated Vps53 1-624. As expected, full-length Vps53 rescued the normal TGN localization of TGN46 (Fig. 8C) in the majority of transfected cells (92%; $n = 296$), whereas truncated Vps53 did so in only a small fraction of cells (2.8%; $n = 235$) (Fig. 8C). As expected, the Vps53 Δ57-95 construct, which lacks the ability to bind Vps54 and SNAREs (Fig. 2D), was nonfunctional in the rescue experiments (data not shown). However, overexpression of this inactive protein did not show any dominant-negative effect (data not shown), indicating that this also requires the ability to assemble with Vps54, to interact with SNAREs, and/or to localize to the TGN. Taken together, these results indicate that GARP-SNARE interactions are necessary but not sufficient to promote retrograde transport to the TGN. Therefore, GARP might participate in tethering by recognition of factors other than SNAREs through the C-terminal domain of Vps53.

**GARP binding to retrograde transport intermediates requires the C-terminal region of Vps53.** Because the tethering function of GARP has never been demonstrated in vitro, we tested the ability of immobilized GARP complex to interact with retrograde transport intermediates. Recombinantly expressed Vps52-Vps53-Vps54 complex was purified on Strep-Tactin–Sepharose beads as in Fig. 3A and used as the solid phase. To generate a pool of retrograde transport intermediates, HeLa cells were depleted of Vps52 and transfected with Vamp4-GFP cDNA, and the pool of light transport intermediates that accumulated in the absence of GARP was isolated by glycerol gradient centrifugation as in Fig. 6A. We found that a significant fraction of Vamp4-GFP-containing vesicles specifically bound to beads containing purified GARP in a concentration-dependent manner (Fig. 8D, lanes 3 to 4) but not a GARP complex consisting of Vps52, Vps53 1-624, and Vps54 (Fig. 8D, lanes 1 and 2). These results correlated with the loss of function observed in vivo for the Vps53 1-624 mutant. Therefore, the ability of GARP to bind transport intermediates requires the C-terminal region of Vps53.

## DISCUSSION

Herein we report novel, specific interactions between the mammalian GARP complex and components of the Stx6/Stx16/Vamp4/Vti1a SNARE complex involved in retrograde transport from endosomes to the TGN. We show that these interactions promote assembly of the SNARE complex, enabling transport of retrograde cargo to the TGN. In addition, we demonstrate for the first time the ability of GARP to bind retrograde transport intermediates, consistent with its proposed activity as a tethering factor. Remarkably, the SNARE binding and tethering activities of GARP are separable, requiring the N-terminal and C-terminal parts, respectively, of the Vps53 GARP subunit.

**Two modes of interaction of GARP with SNAREs.** We found that mammalian GARP subunits bind to the regulatory Habc domain of Stx6 (Fig. 2B and C). This interaction resembles the situation in yeast, in which a short helix (residues 18 to 30) from Vps51p interacts with the Habc domain of the t-SNARE Tlg1p (5, 32). However, removal of the Tlg1p interaction domain from Vps51p does not cause any defect in trafficking (8), questioning the functional relevance of this interaction. This suggests the existence of alternative mechanisms for GARP-SNARE interactions. Indeed, we found a second mode of interaction in which the mammalian GARP complex binds via the N-terminal, coiled-coil-containing domains of Vps53 and Vps54 to the SNARE motifs of Stx6, Stx16, and Vamp4 (Fig. 2). These coiled-coil domains exhibit low but significant homology to domains found in components of the COG and exocyst complexes (44). It has been proposed that these conserved structural elements might have common functions or be responsible for the assembly of each complex (44). Here we demonstrate that the short coiled-coil region containing amino acids 57 to 96 of Vps53 is indeed necessary for assembly with Vps54, as well as for interaction with the SNARE motif (Fig. 2D). It is thus tempting to suggest that a common function of the coiled-coil domains of quatrefoil tethers is binding to SNARE motifs. In fact, binding of the COG complex to Stx5 is mediated, at least in part, by the 220 N-terminal amino acids of the COG4 subunit (29), which encompass several small coiled-coils (44).

Other tethers have also been shown to bind to the SNARE motif. For example, p115 interacts with the SNARE motifs of the cognate t-SNARE Stx5 and v-SNARE GOS28 (30). The

24 h after this final transfection, double labeled with antibodies to the indicated proteins followed by secondary antibodies, and analyzed by confocal immunofluorescence microscopy. Notice that the normal localization of TGN46 was recovered only in those cells expressing full-length Vps53 but not the deleted mutant (arrows). Bars, 10 μm. (D) Purified full-length recombinant GARP, but not GARP containing the Vps53(1-624) mutant, is able to bind retrograde cargo vesicles in an in vitro tethering experiment. Vamp4-GFP-containing vesicles were incubated with serial dilutions of purified full-length or mutant GARP immobilized on Strep-Tactin beads as indicated on the top of the figure. Binding of vesicles was monitored by immunoblotting of SDS-PAGE-separated proteins with antibody to GFP. A negative control with beads incubated with extract from untransfected HeLa cells was also included. Data are representative of three independent experiments with similar results.

COG complex also binds the SNARE motif of several SNAREs, most prominently Stx5 (29). It is remarkable that, despite the promiscuity in the assembly of SNARE proteins, and particularly of the coiled-coil SNARE motifs (12), all of these tethering factors, including GARP, are able to discriminate between different SNAREs, highlighting the exquisite specificity of tether-SNARE interactions (29, 30). COG and p115 specifically bind SNAREs involved in Golgi complex-to-endoplasmic reticulum traffic, whereas GARP binds SNAREs of the endosome-to-TGN pathway. One interesting possibility is then that the selective specificity of SNARE pairing in vivo is conferred, at least in part, from their previous recognition by tethering factors.

**GARP binds to both individual SNAREs and assembled SNARE complexes.** Our results showed that GARP can bind to both individual SNAREs and assembled SNARE complexes (Fig. 3D). This binding is specific for SNAREs involved in endosome-to-TGN transport (Fig. 1) and strong enough to withstand washing in pull-down and immunoprecipitation assays (Fig. 1 to 4). This specificity is consistent with the function of the SNARE complex formed by Stx16, Stx6, Vti1a, and Vamp4 at the TGN interface, as initially shown by Mallard and colleagues (15). In contrast to Vamp4, the closely related Vamp3 bound very weakly to GARP (~25-fold lower than Vamp4 [Fig. 1B]). Although Vamp3 has also been previously implicated in the retrograde route for both Shiga toxin B subunit (15) and CI-MPR (9, 15), our data suggest that Vamp4 is the cognate v-SNARE for Stx6/Stx16/Vti1a in connection to GARP. Because Vamp3 has also been implicated in early endosome fusion reactions and recycling toward the plasma membrane (22), we think that it might participate in events upstream of TGN tethering. In line with these findings, Vamp4, together with Stx6 and Stx16, has been implicated in vesicular trafficking of low-density lipoprotein-derived cholesterol from endosomes to the endoplasmic reticulum via the TGN (41).

The ability of GARP to bind indistinctly to single SNAREs and SNARE complexes indicates that it might directly participate in the assembly and subsequent stabilization of SNARE complexes. In support of such a role, depletion of GARP subunits by RNAi decreased formation of the Stx6/Stx16/Vti1a/Vamp4 SNARE complex in vivo (Fig. 5). Other potential explanations, however, cannot be ruled out. For example, GARP might concentrate SNAREs in areas of the membrane where tethering, and later fusion, takes place. Such a mechanism has been proposed for the tether EEA1 and the SNARE Stx13 in early endosomes. Both proteins are part of large oligomers that mark the sites and provide the machinery for membrane fusion (16). Finally, some of the effects of GARP on SNARE assembly could be indirect. Indeed, GARP knockdown interrupts the normal cycling of TGN SNAREs between endosomes and the TGN, resulting in their accumulation within retrograde transport intermediates and consequent depletion from the TGN (Fig. 6). These effects, however, do not explain why the TGN SNAREs fail to assemble, since they are all contained within the same retrograde transport intermediates. Furthermore, depletion of Rab7, which partially blocks retrograde transport between endosomes and the TGN (24, 28), did not affect SNARE assembly at this level, even though the recycling of Vamp4-GFP from the plasma membrane was clearly altered (Fig. 7). A direct effect of GARP on SNARE complex formation therefore remains the most likely, though not the only, explanation of this phenotype. In vitro SNARE assembly studies, requiring larger quantities of recombinant GARP than those used here, will be needed to test this effect directly.

The COG and HOPS tethers can also bind to SNARE complexes (29, 36), which is in line with our findings for the GARP complex. HOPS, in particular, participates in the cycle of SNARE/HOPS/NSF-α-SNAP binding events that take place during homotypic fusion of yeast vacuoles (3). In this context, HOPS promotes SNARE complex assembly and proofreads its structure (36), eventually being displaced by NSF and α-SNAP, which disassemble the SNARE complex for further rounds of fusion (3).

**Separate SNARE assembly and tethering functions of GARP.** Tethering factors are thought to have multiple roles both before and after the recognition of incoming vesicles. Since many of the tethers display physical interactions with SNAREs, it has been suggested that SNAREs might be the vesicular "postal codes" recognized by tethers to bind incoming vesicles (38). Our results suggest that the actual mechanism for the GARP complex is more complex. Indeed, we found that a C-terminal deletion in Vps53 prevents binding of retrograde transport intermediates by GARP (Fig. 8D) but not its interaction with SNAREs (Fig. 2D). Accordingly, overexpression of Vps53 1-624 elicits a dominant negative effect (Fig. 8A), resembling the phenotype observed upon GARP depletion (Fig. 8C). Since Vps53 1-624 assembles properly into the GARP complex (Fig. 2D) and localizes to the TGN (Fig. 8A), its loss-of-function phenotype implies that the C-terminal region acts prior to the commitment to the SNAREs, most likely in the initial tethering of retrograde transport intermediates. In support of this notion, an immobilized form of GARP bearing a C-terminally truncated Vps53 is unable to specifically bind retrograde transport intermediates, unlike the full-length complex (Fig. 8D). Therefore, GARP must recognize factors other than SNAREs in the performance of its tethering function, implying that the GARP-SNARE interaction is not essential for the tethering process itself but most likely for the activation of the downstream fusion machinery.

Two separate roles of GARP are thus apparent: tethering and promotion of SNARE complex assembly. These roles clearly position GARP upstream of SNAREs in the chain of events leading to membrane fusion and are consistent with a model in which tethering factors provide both specificity and efficiency to the fusion process.

## ACKNOWLEDGMENTS

We thank X. Zhu and H.-I. Tsai for expert technical assistance and W. Sundquist for the kind gift of reagents.

This work was funded by the Intramural Program of NICHD of the NIH. F.J.P.-V. was the recipient of a postdoctoral fellowship from the Ministerio de Educación y Ciencia of Spain.

## REFERENCES

1. **Behnia, R., and S. Munro.** 2005. Organelle identity and the signposts for membrane traffic. Nature **438:**597–604.
2. **Bonifacino, J. S., and B. S. Glick.** 2004. The mechanisms of vesicle budding and fusion. Cell **116:**153–166.
3. **Collins, K. M., N. L. Thorngren, R. A. Fratti, and W. T. Wickner.** 2005. Sec17p and HOPS, in distinct SNARE complexes, mediate SNARE complex disruption or assembly for fusion. EMBO J. **24:**1775–1786.

4. **Conboy, M. J., and M. S. Cyert.** 2000. Luv1p/Rki1p/Tcs3p/Vps54p, a yeast protein that localizes to the late Golgi and early endosome, is required for normal vacuolar morphology. Mol. Biol. Cell **11:**2429–2443.
5. **Conibear, E., J. N. Cleck, and T. H. Stevens.** 2003. Vps51p mediates the association of the GARP (Vps52/53/54) complex with the late Golgi t-SNARE Tlg1p. Mol. Biol. Cell **14:**1610–1623.
6. **Conibear, E., and T. H. Stevens.** 2000. Vps52p, Vps53p, and Vps54p form a novel multisubunit complex required for protein sorting at the yeast late Golgi. Mol. Biol. Cell **11:**305–323.
7. **Drin, G., V. Morello, J. F. Casella, P. Gounon, and B. Antonny.** 2008. Asymmetric tethering of flat and curved lipid membranes by a golgin. Science **320:**670–673.
8. **Fridmann-Sirkis, Y., H. M. Kent, M. J. Lewis, P. R. Evans, and H. R. Pelham.** 2006. Structural analysis of the interaction between the SNARE Tlg1 and Vps51. Traffic **7:**182–190.
9. **Ganley, I. G., E. Espinosa, and S. R. Pfeffer.** 2008. A syntaxin 10-SNARE complex distinguishes two distinct transport routes from endosomes to the trans-Golgi in human cells. J. Cell Biol. **180:**159–172.
10. **Hanson, P. I., R. Roth, H. Morisaki, R. Jahn, and J. E. Heuser.** 1997. Structure and conformational changes in NSF and its membrane receptor complexes visualized by quick-freeze/deep-etch electron microscopy. Cell **90:**523–535.
11. **Hayes, G. L., F. C. Brown, A. K. Haas, R. M. Nottingham, F. A. Barr, and S. R. Pfeffer.** 2009. Multiple Rab GTPase binding sites in GCC185 suggest a model for vesicle tethering at the trans-Golgi. Mol. Biol. Cell **20:**209–217.
12. **Jahn, R., and R. H. Scheller.** 2006. SNAREs: engines for membrane fusion. Nat. Rev. Mol. Cell Biol. **7:**631–643.
13. **Liewen, H., I. Meinhold-Heerlein, V. Oliveira, R. Schwarzenbacher, G. Luo, A. Wadle, M. Jung, M. Pfreundschuh, and F. Stenner-Liewen.** 2005. Characterization of the human GARP (Golgi associated retrograde protein) complex. Exp. Cell. Res. **306:**24–34.
14. **Lin, R. C., and R. H. Scheller.** 1997. Structural organization of the synaptic exocytosis core complex. Neuron **19:**1087–1094.
15. **Mallard, F., B. L. Tang, T. Galli, D. Tenza, A. Saint-Pol, X. Yue, C. Antony, W. Hong, B. Goud, and L. Johannes.** 2002. Early/recycling endosomes-to-TGN transport involves two SNARE complexes and a Rab6 isoform. J. Cell Biol. **156:**653–664.
16. **McBride, H. M., V. Rybin, C. Murphy, A. Giner, R. Teasdale, and M. Zerial.** 1999. Oligomeric complexes link Rab5 effectors with NSF and drive membrane fusion via interactions between EEA1 and syntaxin 13. Cell **98:**377–386.
17. **Morita, E., V. Sandrin, S. L. Alam, D. M. Eckert, S. P. Gygi, and W. I. Sundquist.** 2007. Identification of human MVB12 proteins as ESCRT-I subunits that function in HIV budding. Cell Host Microbe **2:**41–53.
18. **Novick, P., C. Field, and R. Schekman.** 1980. Identification of 23 complementation groups required for post-translational events in the yeast secretory pathway. Cell **21:**205–215.
19. **Peplowska, K., D. F. Markgraf, C. W. Ostrowicz, G. Bange, and C. Ungermann.** 2007. The CORVET tethering complex interacts with the yeast Rab5 homolog Vps21 and is involved in endo-lysosomal biogenesis. Dev. Cell **12:**739–750.
20. **Pérez-Victoria, F. J., G. A. Mardones, and J. S. Bonifacino.** 2008. Requirement of the human GARP complex for mannose 6-phosphate-receptor-dependent sorting of cathepsin D to lysosomes. Mol. Biol. Cell **19:**2350–2362.
21. **Pfeffer, S. R.** 2001. Rab GTPases: specifying and deciphering organelle identity and function. Trends Cell Biol. **11:**487–491.
22. **Proux-Gillardeaux, V., R. Rudge, and T. Galli.** 2005. The tetanus neurotoxin-sensitive and insensitive routes to and from the plasma membrane: fast and slow pathways? Traffic **6:**366–373.
23. **Reggiori, F., C. W. Wang, P. E. Stromhaug, T. Shintani, and D. J. Klionsky.** 2003. Vps51 is part of the yeast Vps fifty-three tethering complex essential for retrograde traffic from the early endosome and Cvt vesicle completion. J. Biol. Chem. **278:**5009–5020.
24. **Rojas, R., T. van Vlijmen, G. A. Mardones, Y. Prabhu, A. L. Rojas, S. Mohammed, A. J. Heck, G. Raposo, P. van der Sluijs, and J. S. Bonifacino.** 2008. Regulation of retromer recruitment to endosomes by sequential action of Rab5 and Rab7. J. Cell Biol. **183:**513–526.
25. **Rothman, J. E.** 1996. The protein machinery of vesicle budding and fusion. Protein Sci. **5:**185–194.
26. **Schmidt, T. G., and A. Skerra.** 2007. The Strep-tag system for one-step purification and high-affinity detection or capturing of proteins. Nat. Protoc. **2:**1528–1535.
27. **Schmitt-John, T., C. Drepper, A. Mussmann, P. Hahn, M. Kuhlmann, C. Thiel, M. Hafner, A. Lengeling, P. Heimann, J. M. Jones, M. H. Meisler, and H. Jockusch.** 2005. Mutation of Vps54 causes motor neuron disease and defective spermiogenesis in the Wobbler mouse. Nat. Genet. **37:**1213–1215.
28. **Seaman, M. N., M. E. Harbour, D. Tattersall, E. Read, and N. Bright.** 2009. Membrane recruitment of the cargo-selective retromer subcomplex is catalysed by the small GTPase Rab7 and inhibited by the Rab-GAP TBC1D5. J. Cell Sci. **122:**2371–2382.
29. **Shestakova, A., E. Suvorova, O. Pavliv, G. Khaidakova, and V. Lupashin.** 2007. Interaction of the conserved oligomeric Golgi complex with t-SNARE Syntaxin5a/Sed5 enhances intra-Golgi SNARE complex stability. J. Cell Biol. **179:**1179–1192.
30. **Shorter, J., M. B. Beard, J. Seemann, A. B. Dirac-Svejstrup, and G. Warren.** 2002. Sequential tethering of Golgins and catalysis of SNAREpin assembly by the vesicle-tethering protein p115. J. Cell Biol. **157:**45–62.
31. **Siniossoglou, S., and H. R. Pelham.** 2001. An effector of Ypt6p binds the SNARE Tlg1p and mediates selective fusion of vesicles with late Golgi membranes. EMBO J. **20:**5991–5998.
32. **Siniossoglou, S., and H. R. Pelham.** 2002. Vps51p links the VFT complex to the SNARE Tlg1p. J. Biol. Chem. **277:**48318–48324.
33. **Sinka, R., A. K. Gillingham, V. Kondylis, and S. Munro.** 2008. Golgi coiled-coil proteins contain multiple binding sites for Rab family G proteins. J. Cell Biol. **183:**607–615.
34. **Sivaram, M. V., J. A. Saporita, M. L. Furgason, A. J. Boettcher, and M. Munson.** 2005. Dimerization of the exocyst protein Sec6p and its interaction with the t-SNARE Sec9p. Biochemistry **44:**6302–6311.
35. **Sollner, T., M. K. Bennett, S. W. Whiteheart, R. H. Scheller, and J. E. Rothman.** 1993. A protein assembly-disassembly pathway in vitro that may correspond to sequential steps of synaptic vesicle docking, activation, and fusion. Cell **75:**409–418.
36. **Starai, V. J., C. M. Hickey, and W. Wickner.** 2008. HOPS proofreads the trans-SNARE complex for yeast vacuole fusion. Mol. Biol. Cell **19:**2500–2508.
37. **Stroupe, C., K. M. Collins, R. A. Fratti, and W. Wickner.** 2006. Purification of active HOPS complex reveals its affinities for phosphoinositides and the SNARE Vam7p. EMBO J. **25:**1579–1589.
38. **Sztul, E., and V. Lupashin.** 2006. Role of tethering factors in secretory membrane traffic. Am. J. Physiol. Cell Physiol. **290:**C11–C26.
39. **Tran, T. H., Q. Zeng, and W. Hong.** 2007. VAMP4 cycles from the cell surface to the trans-Golgi network via sorting and recycling endosomes. J. Cell Sci. **120:**1028–1041.
40. **Ungar, D., T. Oka, E. E. Brittle, E. Vasile, V. V. Lupashin, J. E. Chatterton, J. E. Heuser, M. Krieger, and M. G. Waters.** 2002. Characterization of a mammalian Golgi-localized protein complex, COG, that is required for normal Golgi morphology and function. J. Cell Biol. **157:**405–415.
41. **Urano, Y., H. Watanabe, S. R. Murphy, Y. Shibuya, Y. Geng, A. A. Peden, C. C. Chang, and T. Y. Chang.** 2008. Transport of LDL-derived cholesterol from the NPC1 compartment to the ER involves the trans-Golgi network and the SNARE protein complex. Proc. Natl. Acad. Sci. USA **105:**16513–16518.
42. **Vassilieva, E. V., and A. Nusrat.** 2008. Vesicular trafficking: molecular tools and targets. Methods Mol. Biol. **440:**3–14.
43. **Whyte, J. R., and S. Munro.** 2001. The Sec34/35 Golgi transport complex is related to the exocyst, defining a family of complexes involved in multiple steps of membrane traffic. Dev. Cell **1:**527–537.
44. **Whyte, J. R., and S. Munro.** 2002. Vesicle tethering complexes in membrane traffic. J. Cell Sci. **115:**2627–2637.
45. **Wuestehube, L. J., R. Duden, A. Eun, S. Hamamoto, P. Korn, R. Ram, and R. Schekman.** 1996. New mutants of Saccharomyces cerevisiae affected in the transport of proteins from the endoplasmic reticulum to the Golgi complex. Genetics **142:**393–406.
46. **Yoshino, A., S. R. Setty, C. Poynton, E. L. Whiteman, A. Saint-Pol, C. G. Burd, L. Johannes, E. L. Holzbaur, M. Koval, J. M. McCaffery, and M. S. Marks.** 2005. tGolgin-1 (p230, golgin-245) modulates Shiga-toxin transport to the Golgi and Golgi motility towards the microtubule-organizing centre. J. Cell Sci. **118:**2279–2293.
47. **Zolov, S. N., and V. V. Lupashin.** 2005. Cog3p depletion blocks vesicle-mediated Golgi retrograde trafficking in HeLa cells. J. Cell Biol. **168:**747–759.